

Perturbative solution to the SIS epidemic on networks

Lloyd P. Sanders,^{*} Bo Söderberg,[†] Dirk Brockmann,[‡] and Tobias Ambjörnsson[†]

Herein we provide a closed form perturbative solution to a general M -node network SIS model using the transport rates between nodes as a perturbation parameter. We separate the dynamics into a short-time regime and a medium/long-time regime. We solve the short-time dynamics of the system and provide a limit before which our explicit, analytical result of the first-order perturbation for the medium/long-time regime is to be employed. These stitched calculations provide an approximation to the full temporal dynamics for rather general initial conditions.

To further corroborate our results, we solve the mean-field equations numerically for an infectious SIS outbreak in New Zealand (NZ, *Aotearoa*) recomposed into 23 subpopulations where the virus is spread to different subpopulations via (documented) air traffic data, and the country is internationally quarantined. We demonstrate that our analytical predictions compare well to the numerical solution.

INTRODUCTION

In mathematical epidemiology the canonical deterministic susceptible-infected-susceptible (SIS) model is one of the most elementary compartmental models, receiving consistent attention (the specifics of which are given at length below) since the seminal work of Kermack and McKendrick [1]. Put simply, this model partitions a large, well mixed, homogeneous population into two compartments: susceptible and infected, where birth and death are neglected. A susceptible may become infected upon contact with another infected with some finite probability, and conversely an infected will recover after some typical time, becoming once more susceptible.

The simplicity of this model and its ability to characterize the main motifs of viral infections, where recovery does not assure immunity (for example Gonorrhoea [2] or Chlamydia [3]), has allowed for extensive research. Due to the mathematical tractability of the mean-field model, many extensions have been applied, to include other important dynamical factors [4–6]. Although these models have focused on deterministic mean-field approaches as we shall herein, there is also a surge in converting the models over to their stochastic counterparts [7], and analyzing different properties of the system (for a recent example see [8]).

Recently, network theory [9] has sought to understand the large scale realism of human mobility [10, 11], and in turn comprehend the etiology of epidemics on these systems [12]. In a similar vein, researchers have incorporated the concept of metapopulations [13] (a population of populations where in each, mean-field equations suffice to describe the system dynamics) into theoretical epidemiology [14] (for interesting recent examples see [15] and [16]).

These similar directions of spatial structure incorporation have naturally been applied to SIS models on networks [17–19], and metapopulations [20, 21]. From these studies and the current zeitgeist of the field, the current state of the research has implied two salient points: computational power is easily accessible, and the network

epidemic modeling is not readily amenable to classical mathematical tools. In this article address these topics, whereby we amalgamate the SIS model with the current impetus toward network/metapopulation modeling through the use of perturbation theory, to quantify the effects of human mobility on an arbitrary network. We show that certain mathematical tools can be brought to bear on epidemic network models yielding accurate analytical approximations to the full temporal dynamics, which are substantiated by the corresponding numerical simulations.

Within the following section we review the analytics of the canonical single-node SIS model, after which we segregate the population into an M -node network, whereupon the SIS infection is introduced separately to each. We present a closed-form recursive perturbative solution to the network model; therefrom we calculate explicitly the first-order perturbation leading to our study's main result Eq. (17). We generalize our result further by analytically solving the short-time dynamics of the network given arbitrary initial conditions, Eq. (20), and stitching these to the perturbative solution to yield a full-time approximation to the whole network. Subsequently we compare our result to a test case scenario using real-world population and air traffic data. We then discuss the benefits and limitations of the model and where this work may be applied and built upon.

SIS MODEL

In this section we describe the equations which govern the single- and M -node models and perform analytical analysis where applicable.

Canonical single-node SIS model

The single-city SIS model considers a large, well mixed, population, of size N , in some closed environment where death and birth are neglected. The population is divided

into two compartments: susceptible, S ; and infected, I ; where $N = S + I = \text{constant}$. Both S and I are discrete variables. Susceptibles may become infected from contact with the infected at a rate β , and the infected compartment of the population will lose constituents at a rate γ . The mean-field dynamics of each state is then described by the set of equations:

$$\partial_t S(t) = -\frac{\beta}{N}SI + \gamma I, \quad (1)$$

$$\partial_t I(t) = \frac{\beta}{N}SI - \gamma I, \quad (2)$$

where initial conditions are: $S(t = t_0) = S_0 > 0$, and $I(t = t_0) = I_0 > 0$. One immediately notes that $\partial_t [S(t) + I(t)] = 0$, which then ensures that the total population, N , is constant for all time. It is noted that in the mean-field equations above, it is implicitly assumed that S and I are treated as continuous variables [2].

The solution to Eq. (2), and in turn Eq. (1), as $S(t) = N - I(t)$, is solved in various texts (for example see [2]), so for brevity, the solution is given ($t \geq t_0$):

$$I(t) = \frac{I_\infty}{1 + Ve^{-\chi(t-t_0)}}, \quad (3)$$

where $\chi = \beta - \gamma$, and $I_\infty = \chi N / \beta$ is the stable or endemic state of the infected population; and $V = I_\infty / I_0 - 1$ [22]. With respect to Eq. (3), for an epidemic to take place (i.e. some finite fraction of the population remains infected in the long-time limit), we require the basic reproductive ratio: $R_0 = \beta / \gamma$ to satisfy $R_0 > 1$ (which will be assumed henceforth).

To incorporate a spatial component to the model let us consider an arbitrary network of subpopulations.

Perturbative solution to the M -node SIS model

We here further the result found in the previous section through incorporation of an implicit spatial component, by stratifying the large population into M subpopulations (a realistic example is shown Fig. 1). Within each subpopulation (which may be regarded as a community, city, or country), the same assumptions stated in the canonical model still hold: the population is sufficiently large, and well mixed. One then allows for mobility between the nodes on the network, where the fraction of persons traveling from city j to i per unit time is given by the transport rate, $\omega_{i \leftarrow j}$.

Upon each node, an SIS virus is introduced, where the i^{th} city has an infectivity rate of β_i , and recovery rate γ_i . The mean-field set of equations that then describe the dynamics are given by

$$\partial_t S_i(t) = -\frac{\beta_i}{N_i}S_i I_i + \gamma_i I_i + \varepsilon \sum_{j=1}^M (w_{i \leftarrow j} S_j - w_{j \leftarrow i} S_i), \quad (4)$$

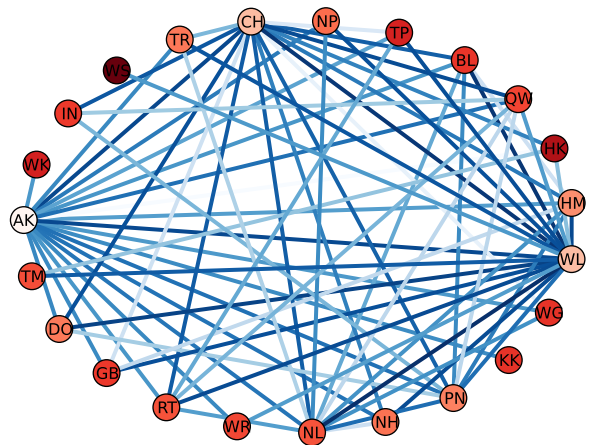


FIG. 1. Abstract representation of the New Zealand air traffic network. Each node (23 total) is an airport which services a region, the lighter the shade the more populated the region (reversal of color scale for label clarity, log-scale). Each link/edge on the graph (70 total) represents a flight connection between airports, the darker the link the more transit between those connections (log-scale) [23]. The network has a diameter of three; with the most connected node Auckland (AK, 19 connections), followed by Christchurch (CH, 18 connections), and Wellington (WL, 16 connections). More information on how this network was constructed is contained in the Appendix, the labels are defined in Tables I and II.

$$\partial_t I_i(t) = \frac{\beta_i}{N_i}S_i I_i - \gamma_i I_i + \varepsilon \sum_{j=1}^M (w_{i \leftarrow j} I_j - w_{j \leftarrow i} I_i). \quad (5)$$

where we have defined $\omega_{i \leftarrow i} = 0$. A convenient parameter $\varepsilon (= 1)$ is introduced here to keep track of the number of times the perturbation enters below (terms which are linear in ε are linear in the travel rates etc) [24]. Summing Eq. (4) and Eq. (5), we find that $\partial_t N_i = 0$, provided that the total influx and outflux for each node are equal, i.e.,

$$\sum_{j=1}^M \omega_{j \leftarrow i} N_i = \sum_{j=1}^M \omega_{i \leftarrow j} N_j, \quad (6)$$

implying the total population N_i of city i is constant for all time. We will assume Eq. (6) to hold henceforth.

To begin the derivation of the perturbative solution, we first assume the influx and outflux of citizens from a given city is small (defined quantitatively later), from there we can define a perturbative solution in terms of the travel rates, namely

$$I_i(t) = \sum_{k=0}^{\infty} \varepsilon^k I_i^{(k)}(t) = I_i^{(0)}(t) + \sum_{k=1}^{\infty} \varepsilon^k I_i^{(k)}(t), \quad (7)$$

where $I_i^{(k)}(t)$ is the k^{th} order contribution to the perturbative expansion at node i ; i.e. $I_i^{(1)}$ contains only linear terms in the transport rates, whereas $I_i^{(2)}(t)$ contains only quadratic terms, and so on. In Eq. (6) $I_i^{(0)}(t)$ is given

by Eq. (3), with replacements $\beta \rightarrow \beta_i$ and $\gamma \rightarrow \gamma_i$ (and therefore $\chi \rightarrow \chi_i$). Explicitly:

$$I_i^{(0)}(t) = \frac{I_{\infty,i}}{1 + V_i e^{-\chi_i(t-t_0)}}. \quad (8)$$

Similarly we can define the perturbative solution to the number of susceptibles in city i as $S_i = \sum_{k=0}^{\infty} \varepsilon^k S_i^{(k)}$. Since $N_i = I_i^{(0)} + S_i^{(0)}$, it follows that $I_i^{(k)} = -S_i^{(k)}$ for $k \geq 1$. Using this fact and substituting Eq. (7) into Eq. (5) and equating factors of ε^k , we find for $k = 0$, that $\partial_t I_i^{(0)} = \chi_i I_i^{(0)} - \frac{\beta_i}{N_i} [I_i^{(0)}]^2$, which is equivalent to Eq. (2), and whose solution is therefore given by Eq. (8). For $k \geq 1$ we obtain our formal perturbation equations

$$\begin{aligned} \partial_t I_i^{(k)} - \left(\chi_i - \frac{2\beta_i I_i^{(0)}}{N_i} \right) I_i^{(k)} = & -\frac{\beta_i}{N_i} \sum_{k'=1}^{k-1} I_i^{(k-k')} I_i^{(k')} \\ & + \sum_{j=1}^M \left(\omega_{i \leftarrow j} I_j^{(k-1)} - \omega_{j \leftarrow i} I_i^{(k-1)} \right), \end{aligned} \quad (9)$$

where we have set $\varepsilon = 1$. Thus, we have formally converted the non-linear problem in Eq. (4) and Eq. (5) into a set of inhomogeneous, linear equations, Eq. (9), with time dependent coefficients. The time dependence of these coefficients in the left-hand-side enters only through the known quantity, $I_i^{(0)}(t)$, whereas the right-hand side depends recursively on the previous perturbation orders.

With regard to the initial condition of the system, the time t_0 , viz. Eq. (8), need not be the true initial time, but rather some time at which $\vec{I}(t) (\equiv [I_1(t), I_2(t), \dots, I_M(t)]^T)$ is known. We will, in a subsequent section, utilize this freedom of choice in t_0 to improve upon the results in this section.

We proceed by expressing a formal solution to Eq. (9) through employment of the integrating factor method. Firstly, we define the so-called integrating factor: $\exp(B_i(t))$, where $B_i(t) = -\int_{t_0}^t [\chi_i - 2\beta_i I_i^{(0)}(t')/N_i] dt'$. Then the formal solution to the k^{th} -order perturbative term is $I_i^{(k)}(t) = \exp(-B_i(t)) \left[\int_{t_0}^t \exp(B_i(t')) g_i^{(k-1)}(t') dt' + G_i^{(k)} \right]$,

where, from the initial conditions: $I_i^{(k)}(t = t_0) = 0$, we have $G_i^{(k)} = 0$. The function $g_i^{(k-1)}(t)$ is defined as

$$\begin{aligned} g_i^{(k-1)}(t) = & -\frac{\beta_i}{N_i} \sum_{k'=1}^{k-1} I_i^{(k-k')} I_i^{(k')} \\ & + \sum_{j=1}^M \left(\omega_{i \leftarrow j} I_j^{(k-1)} - \omega_{j \leftarrow i} I_i^{(k-1)} \right). \end{aligned} \quad (10)$$

Interestingly, we are able to calculate $B_i(t)$ explicitly. Using Eq. (8), we can write $B_i(t) = -\chi_i(t - t_0) + (2\beta_i I_{\infty,i})/(N_i) \int_{t_0}^t (1 + V_i e^{-\chi_i(t'-t_0)})^{-1} dt'$. We solve this to yield the solution $B_i(t) =$

$\ln \left[e^{\chi_i(t-t_0)} \left(\frac{1 + V_i e^{-\chi_i(t-t_0)}}{1 + V_i} \right)^2 \right]$. Using the solution for $B_i(t)$ and Eq. (10) and substituting this into the formal solution given, we explicitly obtain the k^{th} order perturbation, namely

$$\begin{aligned} I_i^{(k)}(t) = & e^{-\chi_i(t-t_0)} \left(1 + V_i e^{-\chi_i(t-t_0)} \right)^{-2} \left[\int_{t_0}^t e^{\chi_i(t'-t_0)} \right. \\ & \left. \times \left(1 + V_i e^{-\chi_i(t'-t_0)} \right)^2 g_i^{(k-1)}(t') dt' \right]. \end{aligned} \quad (11)$$

With this closed form expression, we are able to calculate any order perturbation we require, recursively. Namely, starting from the zeroth-order solution, Eq. (8), we can insert this into Eq. (10), the result of which is then input into Eq. (11) to find the first-order perturbation (shown explicitly in the following section). To find the next order, one uses the first-order result in place of the zeroth-order solution to, following the outlined algorithm, arrive at the second-order perturbation. This operation may be repeated until the desired number of orders are achieved. Then the orders are summed, viz. Eq. (7) (with $\varepsilon = 1$), to gain the final solution to the infected population contained in city i .

Explicit first-order perturbation

Let us now calculate the first order perturbation term $k = 1$. Then the function $g_i^{(0)}$, see Eq. (10), is explicitly: $g_i^{(0)}(t) = \sum_j (\omega_{i \leftarrow j} I_j^{(0)} - \omega_{j \leftarrow i} I_i^{(0)})$, such that Eq. (11), using Eq. (8), becomes

$$I_i^{(1)} = \frac{e^{-\chi_i(t-t_0)}}{(1 + V_i e^{-\chi_i(t-t_0)})^2} \sum_{j=1}^M [\omega_{i \leftarrow j} Q_{ij} - \omega_{j \leftarrow i} Q_{ji}], \quad (12)$$

where

$$Q_{ij} = I_{\infty,j} \int_{t_0}^t e^{\chi_i(t'-t_0)} \frac{(1 + V_i e^{-\chi_i(t'-t_0)})^2}{1 + V_j e^{-\chi_j(t'-t_0)}} dt'. \quad (13)$$

The quantity Q_{ij} may be expressed in terms of hypergeometric functions [25].

For the scope of this manuscript, let us analyze the case where we shall assume that all infection and recovery rate parameters are independent of the city, namely $\beta_i = \beta_j = \beta$ and $\gamma_i = \gamma_j = \gamma$. Explicitly evaluating Eq. (13), we find that

$$\begin{aligned} Q_{ij} = & \frac{-I_{\infty,j}}{\chi} \left[\frac{(V_i - V_j)^2}{V_j} \ln \left(\frac{1 + V_j e^{-\chi(t-t_0)}}{1 + V_j} \right) + 1 \right. \\ & \left. - \chi(t - t_0)(2V_i - V_j) - e^{\chi(t-t_0)} \right]. \end{aligned} \quad (14)$$

This leads to the explicit first-order perturbative contribution to Eq. (7),

$$I_i^{(1)} = \frac{e^{-\chi(t-t_0)}}{\chi(1+V_i e^{-\chi(t-t_0)})^2} \left(\sum_{j=1}^M \omega_{i \leftarrow j} I_{\infty, j} \times \left[\chi(2V_i - V_j)(t-t_0) - \frac{(V_i - V_j)^2}{V_j} \ln \left(\frac{1+V_j e^{-\chi(t-t_0)}}{1+V_j} \right) \right] - \sum_{j=1}^M \omega_{j \leftarrow i} I_{\infty, i} \chi V_i (t-t_0) \right), \quad (15)$$

where we have used Eq. (6). Eqs. (8) and (15), with $I_i(t) = I_i^{(0)}(t) + I_i^{(1)}(t)$ constitute the first-order solution

$$I_i(t) = \frac{I_{\infty, i}}{1+V_i e^{-\chi(t-t_0)}} \left(1 + \frac{e^{-\chi(t-t_0)}}{(1+V_i e^{-\chi(t-t_0)})} \sum_{j=1}^M \frac{\omega_{j \leftarrow i}}{\chi} (V_i - V_j) \left[\chi(t-t_0) - \frac{V_i - V_j}{V_j} \ln \left(\frac{1+V_j e^{-\chi(t-t_0)}}{1+V_j} \right) \right] \right) + \mathcal{O}(w_{i \leftarrow j}^2), \quad (17)$$

where

$$V_i = \frac{I_{\infty, i}}{I_{0, i}} - 1,$$

and

$$I_{\infty, i} = \frac{N_i \chi}{\beta}.$$

The first-order approximation to $I_i(t)$, namely, Eq. (17), is valid when the perturbation due to mobility is “small”. To quantify explicitly the validity of Eq. (17) we introduce the approximate validity indicator:

$$C_i(t_0) = \sum_{j=1}^M \frac{\omega_{j \leftarrow i}}{\chi} |V_i - V_j| = \sum_{j=1}^M \frac{\omega_{j \leftarrow i}}{\beta} \left| \frac{N_i}{I_{0, i}} - \frac{N_j}{I_{0, j}} \right|. \quad (18)$$

For a given system, when $C_i(t_0) \approx 0$ the zeroth-order solution is valid for $I_i(t)$; when $C_i(t_0) \sim \mathcal{O}(1)$ the first-order solution is an accurate approximation to Eq. (5). For $C_i(t_0) \gg 1$, Eq. (17) breaks down. It should be noted that $C_i(t_0)$ may be valid for node i , but the corresponding indicator for some other node j may not be. In this case, Eq. (17) would be reasonable still for $I_i(t)$, but not for $I_j(t)$, therefore caution is advised. In particular we point out that, besides the travel rate $\omega_{j \leftarrow i}$ (in units of β), also the fraction of initially infected for each node enters Eq. (18) in a non-trivial way. Eq. (18) requires that every neighboring node have a finite fraction of initially infected for Eq. (17) to be valid. This stems from the fact that if a node is initially uninfected, the transport of infected persons into that node, see Eq. (5), is no longer

to the SIS epidemic.

If instead of zero net nodal flux, Eq. (6), we instate the more restrictive clause of detailed balance [12], $\omega_{i \leftarrow j} N_j = \omega_{j \leftarrow i} N_i$, we have that $\omega_{i \leftarrow j} I_{\infty, j} = \omega_{j \leftarrow i} I_{\infty, i}$. Using this relation, we can write out the first order perturbation, Eq. (15), explicitly as

$$I_i^{(1)} = \frac{I_{\infty, i} e^{-\chi(t-t_0)}}{\chi(1+V_i e^{-\chi(t-t_0)})^2} \sum_{j=1}^M \omega_{j \leftarrow i} (V_i - V_j) \times \left[\chi(t-t_0) - \frac{V_i - V_j}{V_j} \ln \left(\frac{1+V_j e^{-\chi(t-t_0)}}{1+V_j} \right) \right] \quad (16)$$

Summing this with the zeroth-order solution we reap the first-order perturbative approximation to the number of infected in city i at time t :

small (compared to the infectivity and recovery term), i.e. the base assumption of our perturbative approach is violated, therefore Eq. (17) breaks down. To remedy this initial condition restriction, we turn to linearization of the short-time dynamics in the next subsection.

Short-time approximation

We utilize the prerogative in the choice of t_0 in the previous section in order to generalize Eq. (17). We do this via approximating the short-time regime to allow for any initial state of the system, not only that all nodes be infected as required by the first-order perturbation result. We begin by neglecting the quadratic term $I_i^2 N_i^{-1}$ in Eq. (5) (as it is generally small for short times compared to the linear term), thereby linearizing it to

$$\partial_t I_i(t) \approx \left(\chi - \sum_{j=1}^M \omega_{j \leftarrow i} \right) I_i + \sum_{j=1}^M \omega_{i \leftarrow j} I_j. \quad (19)$$

This can be written as $\partial_t \vec{I}(t) \approx (\mathbf{\Omega} + \mathbf{\chi}) \vec{I}(t)$, where $\Omega_{ij} = \omega_{i \leftarrow j}$ (for $i \neq j$), and $\Omega_{ii} = -\sum_j \omega_{j \leftarrow i}$. For the second matrix, $\mathbf{\chi} = \chi \mathbf{I}$ (\mathbf{I} is the identity matrix). Through the Baker-Campbell-Hausdorff formula, and the commutativity of $\mathbf{\chi}$ and $\mathbf{\Omega}$, the general solution to this set of equations is

$$\vec{I}(t) = \exp(\mathbf{\Omega} t) e^{\chi t} \vec{F}_0, \quad (20)$$

where $\vec{F}_0 = \vec{I}(t=0)$ is the actual initial condition [26]. Note that \vec{F}_0 is different to the initial conditions used for

the first-order perturbation result, i.e. $\vec{I}_0 = \vec{I}(t = t_0)$. In Eq. (20) the zeroth-order dynamics are captured via $\exp(\chi t)\vec{F}_0$, and the correction factor to the zeroth-order, captured in $\exp(\Omega t)$, due to travel.

To find a limiting time for which Eq. (20) is valid, consider the following: we can recast Eq. (20) as

$$\vec{I}(t) = e^{\chi t} \sum_{\alpha} \vec{r}_{\alpha} \exp(\lambda_{\alpha} t) \vec{\ell}_{\alpha} \cdot \vec{F}_0, \quad (21)$$

where the subscript α labels the eigenmode of the eigenvalue (λ_{α}), to the corresponding left ($\vec{\ell}_{\alpha}$) and right (\vec{r}_{α}) eigenvectors of Ω [27]. We can approximate these exact linear dynamics by considering the contribution of only the leading eigenmode, $\alpha_0 = 0$ with $\lambda_0 = 0$ [28]. Then we have $\vec{\ell}_0 = [1, 1, \dots, 1]^T$, and $\vec{r}_0 = N_{\text{tot}}^{-1}[N_1, N_2, \dots, N_M]^T$, where $N_{\text{tot}} = \sum_{j=1}^M N_j$. So, per node, Eq. (21) simplifies to $I_i(t) \approx N_{\text{tot}}^{-1} N_i F_0^{\text{tot}} \exp(\chi t)$, where $F_0^{\text{tot}} = \sum_{j=1}^M F_{0,j}$. We wish to investigate where the linear approximation is valid, by comparing the linear and quadratic terms: $\beta/N_i I_i^2 \ll \chi I_i$, or $I_i \ll N_i \chi \beta^{-1} \equiv I_{\infty,i}$. Using the $\alpha = 0$ linear approximation for I_i (as described above), we get that the linear approximation should be valid for $\exp(\chi t) N_i N_{\text{tot}}^{-1} F_0^{\text{tot}} \ll N_i \chi \beta^{-1}$ where the N_i drops out, leaving us with $\exp(\chi t) \ll (\chi \beta^{-1}) / (F_0^{\text{tot}} / N_{\text{tot}})$ which we recognize as the ratio between the asymptotic fraction of infecteds to the initial one. Thus we expect the linear approximation to break down as this limit saturates, i.e. at

$$t_s = \chi^{-1} \ln[(\chi/\beta) / (F_0^{\text{tot}} / N_{\text{tot}})]. \quad (22)$$

A positive t_s indicates that we need the initial linear stage, before switching to the non-linear dynamics in the perturbative approximation. A negative t_s , on the other hand, indicates that we can skip the linear step, and go directly to the nonlinear stage. Henceforth, t_s will be referred to as the short-time limit.

If we are to "stitch" Eq. (20) to Eq. (17), we require that Eq. (17), be valid, i.e. $C_i(t_0) \sim \mathcal{O}(1)$, where t_0 shall now be known as the stitch time. This criterion sets a soft lower bound to the use of Eq. (20). We establish a cut-off value of the validity indicator to be $C_{\text{cut},i} = C_i(t = t_c) \sim \mathcal{O}(1)$. Then the time-frame for a suitable stitching is $t_c < t_0 < t_s$. This stitched approximation allows us to model the full temporal dynamics of the network irrespective of the initial conditions.

To illustrate Eq. (20) and Eq. (21), we construct a simple system of two nodes, whose the eigenvalues are Ω are $\{\lambda_1, \lambda_2\} = \{0, -(\omega_{1\leftarrow 2} + \omega_{2\leftarrow 1})\}$ (see [28]), with the respective eigenvectors: $\vec{v}_1 = [\omega_{1\leftarrow 2} \omega_{2\leftarrow 1}^{-1}, 1]^T$ and $\vec{v}_2 = [-1, 1]^T$. If we set the initial conditions, $\vec{I}(t = 0) = [F_{0,1}, 0]^T$, then the nodal short-time evolution is: $I_1(t) = F_{0,1} \omega_T^{-1} [\omega_{2\leftarrow 1} \exp(\chi t) + \omega_{1\leftarrow 2} \exp([\chi - \omega_T]t)]$, $I_2(t) = F_{0,1} \omega_{2\leftarrow 1} \omega_T^{-1} [\exp(\chi t) - \exp([\chi - \omega_T]t)]$; where $\omega_T = \omega_{2\leftarrow 1} + \omega_{1\leftarrow 2}$.

SIS EPIDEMIC IN NEW ZEALAND (AOTEAROA)

We proceed by measuring the performance of our analytical expressions, Eq. (17) and Eq. (20), with realistic population [29] and air transport data [30] through a test case scenario, an SIS epidemic in New Zealand (NZ). Firstly, we suppose an infectious virus ($\beta = 0.15 \text{ day}^{-1}$, $\gamma = 0.10 \text{ day}^{-1}$, $R_0 = 1.5$) has introduced itself within the Auckland region (see the Appendix for population statistics) and assume people (and therefore the virus), both susceptible and infected, move between nodes via the air traffic transport network where there is no transport internationally with NZ (which one could think of as a quarantine measure [31]). We consider two networks to illustrate the work done herein, firstly, a simplified model where we recompose NZ into two subpopulations, Auckland, and the remainder of NZ. In the second scenario we consider the full NZ network (as shown in Fig. 1 and described in the Appendix).

NZ two-node system

In the event of an outbreak given the virus parameters mentioned above, we seek to understand how the country's largest city, Auckland (*Tāmaki Makaurau*, subscript "Auck"), is affected and/or affects the remainder of NZ (subscript "rem"). We divide NZ into these two subpopulations (thereby assuming that each of these populations is well mixed). The documented transport rates between these two nodes are $\omega_{\text{rem} \leftarrow \text{Auck}} \approx 5.5 \times 10^{-3} \text{ day}^{-1}$, and $\omega_{\text{Auck} \leftarrow \text{rem}} \approx 3.2 \times 10^{-3} \text{ day}^{-1}$ [23], which are indeed small – as required by our perturbation assumption. We set the initial infected population to $F_{0,\text{Auck}} = 100$, and $F_{0,\text{rem}} = 0$, for Auckland and the remainder of NZ, respectively. Given these initial conditions and virus parameters, the short-time limit is $t_s \approx 200$ days. We use Eq. (20) to model the network until all nodes in the network are infected ($I_i(t) \geq 1, \forall i$), and the validity indicator for Auckland, $C_{\text{Auck}} \leq 2$. At this time ($t_0 \approx 108$ days) we use the state of the system as the initial condition for Eq. (17), and model the remaining infection dynamics for both nodes. We also compare our stitched first-order result to the stitched zeroth-order result (using Eq. (8) and Eq. (20)). This scenario of "no travel" can be likened to a situation of quarantine when all nodes have been found to be infected. It is also a measure of how effective the zeroth-order solution, Eq. (8), is at estimating the time-evolution of the epidemic. The stitched first-order and the stitched zeroth-order perturbation approximations are compared to the numerical solution, $\vec{I}_{\text{num}}(t)$ (calculated by the Runge-Kutta 4th order algorithm) in Fig. 2. We note that, in Fig. 2, our analytical result conforms well to the numerical result, where the absolute residuals ($|\Delta_j(t)|$, see Appendix, Eq. (23)) between

the first-order correction and the zeroth-order are given in the inset. The zeroth-order solution performs poorly at estimating the interim dynamics of the epidemic, especially underestimating the fraction of infected in Auckland.

Full NZ network

To assess further the scope of our perturbation result, we reconstruct the system to include all available airports, giving a total of 23 nodes (see Fig. 1 and the Appendix). For this system we assume the same virus as before, with the same initially infected, whom have been introduced initially to the Auckland node (this again gives a short-time limit of $t_s \approx 200$ days). Again, we use Eq. (20) to simulate the short-time regime until all nodes are infected ($I_i(t) \geq 1, \forall i$), and the validity indicator for Auckland $C_{\text{Auck}} \leq 2$. At this time, $t_0 \approx 127$ days, we use Eq. (17) to model the dynamics given the current state of the system. We plot these results for Auckland compared to the numerical solution and the stitched zeroth order approximation, Eqs. (8) and (20), in Fig. 3.

The choice of t_0 here favors a good validity indicator for Auckland. To understand the repercussion of this on other nodes in the network, alongside the infection dynamics of Auckland in Fig. 3, we have plotted the

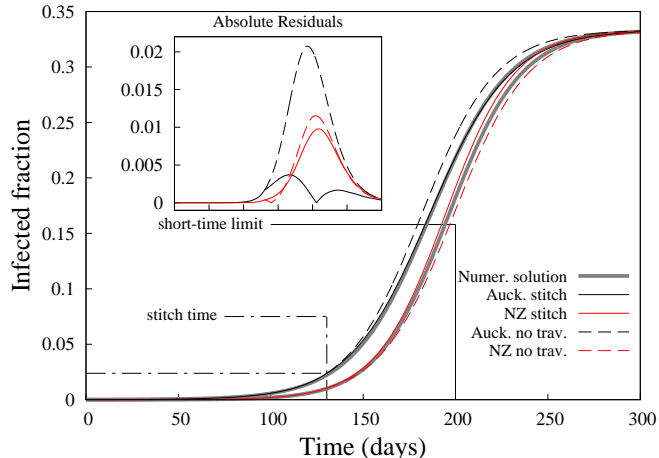


FIG. 2. The infected fraction of the populace over time (due to an SIS epidemic) for each node for an internationally quarantined New Zealand, apportioned into two subpopulations: Auckland, and the remainder of the country. One clearly notes that in both populations, the stitched first-order perturbation, Eq. (17) and Eq. (20) (solid red/black line), approximates the numerical solution well (solid gray line), compared to the stitched zeroth-order solution, Eq. (8) and Eq. (20) (dashed red/black line). INSET: Absolute residuals of the analytical calculations, with respect to the numerical solution. For further explanation and auxiliary parameters see the main text.

dynamics of Timaru (*Te Tahi-o-Maru*). Timaru has the highest validity at the stitch time, $C_{\text{Tim}} \approx 6.39$. This larger validity indicator makes for a worse approximation, as shown in Fig. (3), compared to Auckland with respect to the numerical solution. On the other hand, the stitched zeroth-order fares more poorly given this t_0 . This highlights the subtle consequences in the choice of t_0 .

DISCUSSION AND CONCLUSION

Within this manuscript, we have derived a closed form, recursive, perturbative solution to an SIS epidemic on an arbitrary network, stated in Eqs. (10) and (11). We have proceeded to explicitly calculate the first-order perturbation to the population of infected persons in the i^{th} city as a function of time, to wit, Eq. (17), and then provided a quantitative benchmark under what conditions this solution is accurate: the validity indicator, Eq. (18).

We have generalized Eq. (17), to include the arbitrary initial condition of the network through the linearization of the short-time dynamics, Eq. (20). We quantified a short-time limit, t_s Eq. (22), for which Eq. (20) is valid. The results of Eq. (20) are stitched to Eq. (17), at the stitch time, $t_0 (< t_s)$ (see main text for further remarks). This gives an approximation to the full network dynamics irrespective of initial conditions.

To verify our derived results we simulated an SIS epidemic on an internationally quarantined New Zealand (see Fig. 1). This comparison served a two-fold objective;

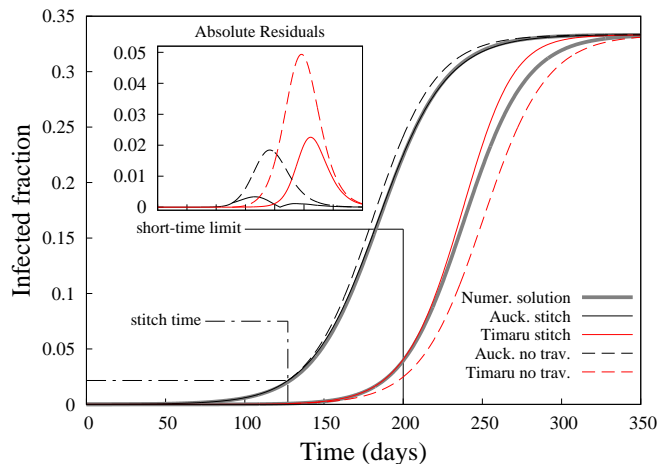


FIG. 3. Infected fraction over time for the Auckland and Timaru regions of an internationally quarantined NZ - illustrated in Fig. 1. These data demonstrate the capabilities of the stitched first-order perturbation, Eq. (17) and Eq. (20) (solid red/black line), on a realistic network (23 airport nodes of NZ, see Appendix) compared to the numerical solution (solid gray line). For further explanation and auxiliary parameters see the main text.

firstly the use of documented air traffic data [32] showed that in this medium of transport, our base assumption: transport rates between communities are small, is indeed reasonable and accurate as a perturbation parameter. Secondly, it serves to show the extent of use of our stitched first-order result; namely that it performs well on a realistic, moderately sized (23 nodes) network.

The derivation makes no assumptions on the type of the network, whether it be a real-world network, regular lattice, a random E-R graph, or a scale-free network [9]. It has also only assumed, besides the detailed balance condition (see Eq. (15) for an expression without this assumption), that the population of each node is large enough such that the mean-field nature of Eq. (3) is true. Therefore the nodes may be seen as communities or countries, rather than only cities. This generality is advantageous for future investigations of SIS epidemics on complex networks/metapopulations as this work may be used in parallel as a confidence measure. But caution is advised. The success of the stitch approximation on this network is due to the magnitude of the travel rates and the diameter of the network. The NZ network has a low diameter of three, with reasonable travel rates, so in turn the short-time approximation is able to "seed" every node, enough so that $C_{\text{Auck}}(t_0) \sim \mathcal{O}(1)$ while $t_0 < t_s$. One could envisage a sparse network with a large diameter and slow travel rates; such that $C_i(t_0) \sim \mathcal{O}(1)$ for $t_s < t_0$. This could then lead to the breakdown of our calculations. So therefore it would be of interest to understand how higher order perturbation terms may regularize our first-order approximation.

One of the striking benefits of the solution is that one has an analytical expression for $I_i(t)$ at all times and as such naturally out-performs usual investigative methods of numerical integration. In this way this solution can be used to gauge parameter sets of large numerical simulations.

These calculations were built upon the assumption of large populations, where mean-field approximations are valid. A natural extension would be the effect of stochasticity for low populations. This may be found through an analytic perturbative solution of the associated master equation akin to that defined for an SIR epidemic in the work of Hufnagel et al. [33].

Although the analytics have been developed under the guise of epidemic modeling, this mathematical framework may be conveniently adopted by other interdisciplinary fields with population growth and metapopulation structure, for example Theoretical Ecology and the concept of island colonization [34].

In conclusion, we hope the mathematical framework determined herein will shift part of the academic interest of epidemics on networks from large scale numerical simulations back to the bedrock of analytical analysis.

The authors would like to thank Erik Lagerstedt, Olivia Woolley-Meza, Sigurður Æ. Jónsson, and for stim-

ulating discussions and the reviewers for constructive criticism regarding the work herein.

Appendix

Within the Appendix we offer more statistics on our analysis of the epidemic on the full NZ network, and instructions on how the network was constructed from census and air traffic data.

NZ Network Statistics

In the full system Eqs. (17) and (20) model the dynamics well for Auckland and Timaru, in comparison to Eqs. (8) and (20) (as shown in Fig. 3), but we seek the performance over the entire network. Due to the size of the system, we have opted to show the residue statistics as a measure of performance over all nodes. We define the residue of node j as

$$\Delta_j(t) = I_j(t) - I_{\text{num},j}(t), \quad (23)$$

where $I_j(t)$ is either the first-order solution or the zeroth-order. The mean residue is then $\bar{\Delta}(t) = M^{-1} \sum_{j=1}^M \Delta_j(t)$; and the standard deviation is $\sigma_{\Delta}(t) = \sqrt{M^{-1} \sum_j (\Delta_j - \bar{\Delta})^2}$. We see holistically in Fig. 4 that the first-order performs better than the zeroth-order solution, on average, for this system.

NZ Network Construction and Parameters

For the case study within this manuscript, NZ has been recomposed into 23 nodes, each identified by the airport which services the node. Each node is constructed through a combination of the census data [29] and air traffic data [32]. The explicit population of each node is shown in Tables I and II. The node is composed of census defined "regions" (numbering 66), and how each census region is billeted to which airport is defined through the following criteria: 1) if a region has only one airport, that airport services the region; 2) If a region has two or more airports, the total influx/outflux of those airports are combined to make one airport node (e.g. Kaitai-Kerikeri); 3) if a region has no airports, and several adjacent airports, the largest airport services that region; 4) all other situations are made on a case by case basis and are highlight via '*' in Tables I and II. The travel rates between nodes are described in Ref. [23].

* Corresponding author: lloyd.sanders@thep.lu.se; Department of Astronomy and Theoretical Physics, Lund University, SE-223 62 Lund, Sweden

† Department of Astronomy and Theoretical Physics, Lund University, SE-223 62 Lund, Sweden

‡ Northwestern Institute on Complex Systems and Department of Engineering Sciences and Applied Mathematics, Northwestern University, Evanston, IL, USA

- [1] W. O. Kermack and A. G. McKendrick, Proceedings of the Royal Society A: Mathematical, Physical and Engineering Sciences **115**, 700 (1927)
- [2] H. W. Hethcote, in *Three basic epidemiological models*, Applied Mathematical Ecology, Vol. 18 (Springer Berlin Heidelberg, 1989) pp. 119–142
- [3] K. M. E. Turner, E. J. Adams, N. Gay, A. C. Ghani, C. Mercer, and W. J. Edmunds, Theoretical biology & medical modelling **3**, 3 (2006)
- [4] J. Llibre and C. Valls, Journal of Mathematical Analysis and Applications **344**, 574 (2008)
- [5] P. Das, Z. Mukandavire, C. Chiyaka, A. Sen, and D. Mukherjee, Differential Equations and Dynamical Systems **17**, 393 (2010)
- [6] V. Méndez, D. Campos, and W. Horsthemke, Physical Review E **86** (2012)
- [7] D. T. Gillespie, Annual review of physical chemistry **58**, 35 (Jan. 2007)
- [8] M. J. Keeling and J. V. Ross, Journal of the Royal Society, Interface / the Royal Society

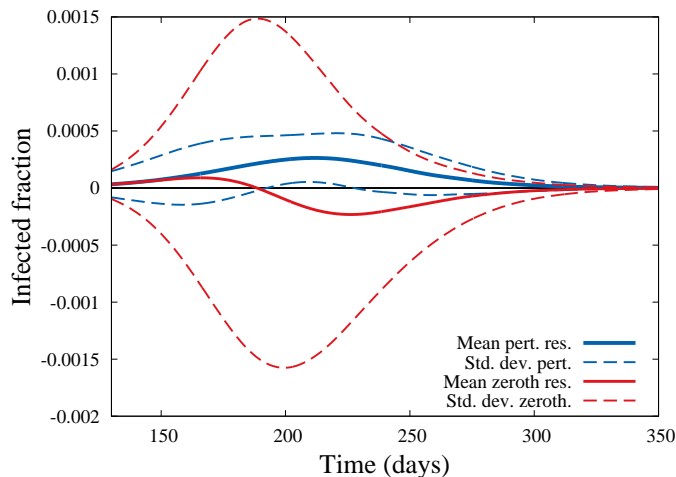


FIG. 4. Illustrated above are the residue statistics as a measure of performance of the first and zeroth order approximations in comparison to the numerical solution (see also Fig. 3 for more information). Plotted is $\bar{\Delta}(t) \pm \sigma_{\Delta}(t)$ of the NZ network (Tables I and II), given a virus $R_0 = 1.5$, $\beta = 0.15$ day $^{-1}$, initially introduced to Auckland, $F_{\text{Auck}}(0) = 100$. The measurement is conducted at the time of stitching, the time at which the epidemic has spread to all nodes ($I_i(t) > 1, \forall i$), and the validity indicator, Eq. (18), for Auckland is $C_{\text{Auck}} \leq 2$. The ordinate axis shows the fraction of the total population.

- 5**, 171 (Feb. 2008)
- [9] M. E. J. Newman, SIAM Review **45**, 167 (2003)
- [10] O. Woolley-Meza, C. Thiemann, D. Grady, J. Lee, H. Seebens, B. Blasius, and D. Brockmann, The European Physical Journal B - Condensed Matter and Complex **1**(2011)
- [11] J. P. Bagrow and Y.-R. Lin, PloS one **7**, e37676 (2012)
- [12] D. Brockmann, in *Reviews of Nonlinear Dynamics and Complexity*, edited by H. G. Schuster (Wiley-VCH, 2009) pp. 1–24, ISBN 9783527408504
- [13] I. Hanski, Nature **396**, 41 (1998)
- [14] B. Grenfell and J. Harwood, Trends in ecology & evolution **19**(1998)
- [15] H. Lund, L. Lizana, and I. Simonsen, Journal of Statistical Physics **151**, 367 (2013)
- [16] V. Colizza and A. Vespignani, Physical Review Letters **99**, 1 (2007)
- [17] R. Parshani, S. Carmi, and S. Havlin, Physical Review Letters **104**, 258701 (Jun. 2010)
- [18] P. Van Mieghem and R. van de Bovenkamp, Physical Review Letters **110**, 108701 (2013)
- [19] S. C. Ferreira, C. Castellano, and R. Pastor-Satorras, Physical Review E **86**, 041125 (2012)
- [20] F. Arrigoni and A. Pugliese, Journal of mathematical biology **45**, 419 (2002)
- [21] F. Ball, Mathematical Biosciences **156**, 41 (1999)
- [22] In Ref. [2] the analytical solution of the SIS model with birth and death is provided. This solution can be used instead of Eq. (3) to yield an approximation to the temporal network dynamics following the derivation used here.
- [23] The air transport rates are calculated from the worldwide air traffic data provided by Ref. [32], taken the same year as the Subnational census data of NZ [29]. We have used the average number of *available* seats (from the total average flights) per day as the measure of the number of people commuting between two airport nodes in the NZ network. The travel weight $\omega_{i \leftarrow j}$ is therefore the people leaving city j as a fraction of N_j . We have also removed all international connections to and from NZ airports.
- [24] J. J. Sakurai, *Modern Quantum Mechanics (Revised Edition)*, 1st ed. (Addison Wesley, 1993) ISBN 0201539292
- [25] M. Abramowitz and I. A. Stegun, *Handbook of Mathematical Functions with Formulas, Graphs, and Mathematical Tables*, 9th ed. (Dover, 1972)
- [26] Using an eigenvalue approach allows us to numerically calculate $\vec{I}(t)$ at any desired (short) time without the need to introduce a time-step, as needed for instance in a Runge-Kutta approach.
- [27] For the case of different infectivity and recovery rates for the different cities, the matrix χ is replaced by a diagonal matrix with elements χ_i . For this case χ and Ω do not commute in general, but the Baker-Campbell-Hausdorff formula still applies. This formula then requires us to evaluate a set of commutation relations in order to get an explicit expression for $\vec{I}(t)$.
- [28] Using the Gershgorin circle theorem [35] for diagonally dominant square matrices, we find that the eigenvalues of Ω in Eq. (20) have the following boundaries: $-2 \max_k S_k \leq \lambda \leq 0$, where S_k defines the sum of rates away from node k , $S_k = \sum_{j \neq k} \omega_{j \leftarrow k}$, or the sum of the column K of Ω .
- [29] Statistics New Zealand, “Subnational Populations Estimates: At 30 June 2011,”

- http://www.stats.govt.nz/browse_for_stats/population/38/Estimates_HOTPJ (2011), [Online; accessed 4-April-2013]
- [30] The transport rates we use [32] satisfy the detailed balance condition, as required for the validity of Eq. (17).
- [31] We consider travel to and from the Chatham islands to be international travel and is therefore omitted.
- [32] OAG, "Air Traffic Data," <http://www.oag.com> (2011), [Data retrieved: 03-Feb-2011]
- [33] *Estimates, projections, and international population estimates*, Proceedings of the National Academy of Sciences of the United States of America **101**, 15124 (2004)
- [34] R. Levins, Bulletin of the Entomological Society of America **15**, 237 (1969)
- [35] S. Gerschgorin, Bulletin de l'Académie des Sciences de l'URSS **6**, 749 (1931)

TABLE I. North Island network of New Zealand. First column defines which airport (with designated label used in Fig. 1) is used by which regions, given in the second column. The third column gives the population for each region, and the fourth is the total population using the corresponding airport.

Node Airport	Regions of Node	Region Pop.	Node Pop.
Kaitai-Kerikeri (KK)	Far North	58500	58500
Whangarei (WR)	Whangarei	80500	80500
Auckland (AK)	Kaipara	119150	1615200
	Auckland city	1486000	
	Hauraki	18750	
	Thames-Coromandal*	27000	
	Waikato	64300	
Hamilton (HM)	Hamilton city	145600	223700
	Matamata-Piako	32000	
	Waipa	46100	
Tauranga (TR)	Tauranga city	115700	161500
	Western BOP	45800	
Rotorua (RT)	Rotorua	68900	91800
	South Waikato	22900	
Whakatane (WK)	Whakatane	34500	41440
	Kawerau	6940	
Gisborne (GB)	Gisborne	46600	63900
	Opotiki	8950	
	Wairoa	8350	
Taupo (TP)	Taupo	34100	43420
	Otorohanga	9320	
New Plymouth (NP)	New Plymouth	73800	132900
	Waitomo	9630	
	Ruapehu	13400	
	Stratford	9170	
	Sth. Taranaki	26900	
Napier-Hastings (NH)	Napier city	57800	146800
	Hastings	75500	
	Centrl Hawkesbay*	13500	
Whanganui (WG)	Whanganui	43500	58300
	Rangitikei	14800	
Palmerston Nrth. (PN)	Palmerston Nrth. city	82100	184000
	Manawatu	30000	
	Tararua	17700	
	Horowhenua	30700	
	Masterton*	23500	
Wellington (WL)	Wellington city	200100	464170
	Kapiti Coast	49800	
	Porirua city*	52700	
	Upperhutt city	41500	
	Lowerhutt city	103000	
	Sth. Wairarapa Carterton	9420 7650	

TABLE II. South Island network of New Zealand. See Table I for discussion of columns.

Node Airport	Regions of Node	Region Pop.	Node Pop.
Nelson (NL)	Nelson city	46200	94300
	Tasman	48100	
Westport (WS)	Buller	10100	10100
Hokitika (HK)	Westland	8960	22860
	Grey	13900	
Christchurch (CH)	Christchurch city	367700	457400
	Waimakariri	48600	
	Selwyn	41100	
Timaru (TM)	Timaru	44700	86480
	Ashburton	30100	
	Mackenzie	4050	
	Waimate	7630	
Queenstown-Wanaka (QW)	Queenstown lakes	28700	76700
	Central Otago	18400	
	Southland	29600	
Blenheim (BL)	Marlborough	45600	60750
	Kaikoura	3850	
	Hurunui	11300	
Dunedin-Oamaru (DO)	Waitaki	20900	164450
	Dunedin city	126000	
	Clutha	17550	
Invercagill (IN)	Invercagill	53000	65300
	Gore*	12300	